ISSN 0915-633X

NATIONAL INSTITUTE FOR FUSION SCIENCE

Effect of Energetic Particle Distribution on Bounce Resonance Excitation of the Ideal Ballooning Mode

T. Yamagishi

(Received – Jan. 11, 1991)

NIFS-75 Feb. 1991

RESEARCH REPORT
NIFS Series

NAGOYA, JAPAN

Effect of Energetic Particle Distribution on Bounce Resonance Excitation of the Ideal Ballooning Mode

Tomejiro Yamagishi

Fukui Institute of Technology, Gakuen, Fukui 910

Abstract

The kinetic effect of energetic trapped particles on the stability of magnetohydrodynamic(MHD) ballooning mode is studied in a tokamak with the circular cross section. The bounce resonance contribution of trapped energetic particles is found to play an important role in the outer inertial region of the ballooning mode perturbation, and destabilizes the ballooning mode when the shear effect is not strong. The inhomogeniety of a model slowing down energetic particle distribution in velocity space, $\partial F/\partial E$, is effective to stabilize the bounce resonant mode.

Keywords: Energetic trapped particles, bounce resonance excitation, averaged ballooning mode equation, tokamak, circular crosssection, inertial range, stabilization by slowing down distribution .

§1. Introduction

Influence of energetic trapped particles on magnetohydrodynamic(MHD) modes have been studies by many authors to find a route to get second stability regime of the ballooning mode, and to interpret experimintal phenomena. Trapped energetic particles on the average over the cental ideal region of ballooning mode perturbation have a zero frequency stationary contribution and stabilizes the ideal ballooning mode[1]. Energetic particles, on the other hand, may make resonant excitation at various characteristic frequencies. Precessional drift resonance excitations of trapped energetic particles combined with the internal kink mode and the ideal ballooning mode may cause the fishbone oscillation[2], and the high frequency MHD oscillation[3], respectively. Untrapped circulating energetic particles may also make a resonance excitation at transit frequency[4].

It is quite natural to think about the possibility of bounce resonance excitation of trapped particles. The bounce resonance contribution, however, is averaged out in the central ideal region of the ballooning mode perturbation , and was completely neglected. When the shear effect is not so strong, the ballooning mode perturbation is not damped out for many toroidal periods along the magnetic field lines, and therefore the trapped particles may feel many times the same perturbation during bounce motion. The bounce resonance contribution may, therefore, survive in the outer inertial region of the ballooning mode perturbation and play an important role as in the case of passing particle resonance[4].

In this paper, we study the bounce resonance problem of trapped energetic particles combined with the MHD balloonig mode in an axisymmetric tokamak with circular cross section. We will use the method of averaged ballooning mode equation[5),6)] which is combined with the kinetic effect of energetic particles derived in a previous paper[4)]. Carefully evaluating the average of the kinetic effect of energetic trapped particles, we actually find that the bounce resonance contribution remains unvanished in the outer inertial region of the ballooning mode perturbation, and play an important role for the bounce resonance excitation. This mode is, however, stabilized when the profile effect of the slowing down distribution function F in the velocity space is not zero, i.e., $\partial F/\partial E \neq 0$ with E being particle energy.

This paper is organized as follows:In §2, carring out the average of the kinetic contribution of energetic trapped particles the averaged balloonig mode equation which involves the kinetic energetic trapped particles effect will be derived. In §3, the dispersion relation will be derived making use of the bouded condition of the ballooning mode eigenfunction. This dispersion relation will be numerically calculated in §4, and the bounce resonance excitation of the ballooning mode will be presented.

§2. Averaged Ballooning Mode Equation

We start with the high n-ballooning mode equation in the axisymmetric toroidal system with the circular cross section:

$$\frac{d}{d\chi} f \frac{d\phi}{d\chi} + (\Omega^2 f + \alpha g)\phi + K(\phi) = 0, \qquad (1)$$

where χ is the extended poloidal-angle-like coordinate $f=1+(s\chi)^2$, $g=\cos\chi+s\chi\sin\chi-\alpha\sin^2\chi-\delta$, $\alpha=\beta' Rq^2$, $\delta=\alpha(1-q^{-2})$, $\varepsilon=r/R$ (r and R being the minor and major radius), $\Omega^2=\omega(\omega-\omega_*^{\,i})/\omega_A^{\,2}$, $\omega_A=v_A/(Rq)$, v_A is the Alfven velocity, $s=rq'/q$ is the shear parameter of the magnetic field lines, $q=rB_z/(RB\chi)$ is the safety factor, and other notations are standard. The kinetic term due to the energetic particles has been given by[4]

$$K(\phi)=\eta g_o(\chi)\int d^3v\omega_d(E)H(\phi), \qquad (2)$$

where $\eta=4\pi\omega e(rR)^2/(in^2c^2)$, $\omega_d(E)=\mathbf{v}_d\cdot\nabla S$, $\mathbf{v}_d=\mathbf{b}\times(v_\perp^{\,2}/2\ln B+v_\parallel^{\,2}\kappa)/\Omega_c$ is the precessional drift velocity of energetic particles and Ω_c is the Larmor frequency. The eikonal function S must satisfies $\mathbf{B}\cdot\nabla S=0$. Since $\mathbf{b}=\mathbf{B}/B$ is the unit tangential vector, and $\kappa=(\mathbf{b}.\nabla)\mathbf{b}$ is its derivative along the magnetic field lines, the curvature $\kappa=|\mathbf{b}\times\mathbf{k}|/\mathbf{b}^3$ of the field line in differential geomertry becomes $\kappa=|\mathbf{b}\times\mathbf{k}|$ which consists of the normal and geodesic curuvaturs which represents the geometrical characteristics of the confinement system, and a key quantity for ballooning stability. The function $H(\chi)$ is the solution of the gyro-kinetic equation. For trapped particles at the resonance condition in the fluid limit, it has been given by eq.(56) in Ref.(4).

Equation (1) involves two different scales when $s<<1$. The short scale $\chi\sim 1$ is related to the toroidal periodicity of the magnetic field lines. The longer scale $z=s\chi>1$ is related to the characteristic decay length of the eigenfunction along the magnetic field lines.

Averaging the eigenfunction ϕ in eq.(1) over the short scale taking into account up to the fourth order of the small parameter α,

we have the distilled differential equation [2)6)7)]:

$$\frac{d}{dz}f\frac{d}{dz}\bar{\phi}-(U_c+\frac{U_1}{1+z^2}+\Lambda_c(1+z^2))\bar{\phi}+\overline{\frac{1}{s^2}K(\bar{\phi})}=0 \quad . \tag{3}$$

The coefficient U_C, U_1 and $\Lambda_C$have been given, for example, as follows

$$U_c=\frac{\alpha}{s^2}(\delta+\frac{3}{128}\alpha^3), \tag{4}$$

$$U_1=(\frac{\alpha}{s})^2(s-\frac{5}{32}\alpha^2), \tag{5}$$

$$\Lambda_c=-(\frac{\Omega}{s})^2, \tag{6}$$

The kinetic contribution from energetie particle, the fourth term in eq.(3), can be separated into the trapped and passing particle contributions:

$$\overline{\frac{1}{s^2}K(\varphi)}=-(U_t+U_p)\bar{\phi}. \tag{7}$$

The trapped particle contributions has been given by eq.(57) in Ref.(4):

$$U_t=-\frac{32\sqrt{2}}{s^2B^2}\pi m_h q^2\int_{(1+\varepsilon)^{-1}}^{1}\frac{d\lambda}{\sqrt{1-\lambda}}(1-\frac{\lambda}{2})^2\int_0^\infty dEE^{\frac{5}{2}}\{\frac{1}{\omega-\bar{\omega}_d}+\sum_{p=1}^{\infty}\frac{2(\omega-\bar{\omega}_d)}{(\omega-\bar{\omega}_d)^2-(p\omega_b)^2}\}$$
$$\overline{Q(g_o(\chi)\cos I(\chi,\chi_-))^2}, \tag{8}$$

where $I(\chi,\chi_-)=\int_{\chi_-}^{\chi}d\chi Rq(\omega-\bar{\omega}_d)|v_{\|}|^{-1}$, and $Q=\omega\partial F/\partial E+(k\chi/\Omega_C)\partial F/\partial r$ is the source of free energy due to the inhomogenieties of F both in the space and velocity space. The passing particle contribution U_p

has been given by eq.(58), and analyzed in some detail in Ref.(4). At the toroidal resonance condition $\omega = \omega_t$ (ω_t being the transit frequency of energetic particles), U_p becomes proportional to $(1+z^2)$. The passing particle contribution U_p, therefore, modifies the inertial coefficient Λ_c in eq.(3). For the sake of simplicity, however, here we neglect this passing particle contribution U_p, and concentrate our attention to the trapped particle contribution U_t at the bounce resonance condition.

First we evaluate the average of $g_o \cos I(\chi,\chi_-)$ in eq.(8). From the definition of the integral $I(\chi,\chi_-)$, we have $I(\chi_+,\chi_-)=\pi(\omega-\omega_d)/\omega_d = \pi p$ ($p=0,1,2,\ $) at the resonance condition and $\partial I(\chi,\chi_-)/\partial\chi = Rq(\omega-\omega_d)/|v_\parallel|$, where $\chi_\pm$ is the turning points of trapped particles at which $v_\parallel = 0$, and $\omega_b = (Rq\oint d\chi/|v_\parallel|)^{-1}$ is the bounce frequency. For $p=0$ ($\omega=\omega_d$) resonance, $I(\chi,\chi_-)=0$ because $\partial I(\chi,\chi_-)/\partial\chi = 0$ in the whole region $[\chi_-,\chi_+]$. In this case, we have $\overline{g_o \cos I(\chi,\chi_-)} = \overline{\cos\chi} = 2E(k)/K(k) - 1$, where K and E are the first and second kind complete elliptic functions, respectively and $k^2=(1-\lambda+\varepsilon\lambda)/(2\varepsilon\lambda)$ with $\lambda=(v_\parallel/v)^2$ as defined in Ref.(4).

Introducing this average for $p=0$ into eq.(8), making use of a model distribution function $F=c(r)E^{-3/2}\delta(\lambda-\lambda_o)$ with $c(r)=p_h/(2^{3/2}E_m m_h \pi K_b)$ and $K_b=\oint d\chi/(2\pi(1-\lambda)^{1/2}) = (2/\varepsilon\lambda)^{1/2}K(k)/\pi$, we obtain the $p=0$ trapped particle contribution from the first term in the curly braces in eq.(8):

$$U_t^{\,o} = w_o\{1+\frac{\omega}{\omega_{dm}}(1-\frac{3\omega_{dm}}{2\omega_{*m}})\log(1-\frac{\omega_{dm}}{\omega})\}, \qquad (9)$$

where $W_o=\pi(q/s)^2\beta_{ht}(\omega_{*m}/\omega_{dm})(2E(k_o)/K(k_o)-1)$ and $\beta_{ht}=8\pi p_h/B^2$, $\omega_{dm}=\omega_d(E_m)$, $\omega_{*m}=\omega_{*h}(E_m)$ and E_m is the maximum energy. In the zero frequency limit $\omega\to 0$, eq.(9) reduces to $U_t^{\,o}=W_o$, i.e., the $p=0$ trapped particle contribution has a stationary zero frequency contribution

which corresponds to the trapped particle effect studied in Ref.(1). The second term which has the logarithmic function plays an important role near the resonance condition $\omega \simeq \overline{\omega_d}$. The factor -3/2 in the second term in eq.(9) which came from $\partial F/\partial E$, plays an significant role for stabilization of the drift resonant branch[8]. Since U_t° has no z, it modifies the Mercier cofficient U_c in eq.(3).

For $p=0$ ($\omega=p\omega_b$) resonance, the derivative $\partial I(\chi,\chi_-)/\partial\chi$ tends to plus infinity, because $v_{\parallel} \to 0$ as $\chi \to \chi_{\pm}$,i,e., $I(\chi,\chi_-)$ sharply increases near the turning points $\chi_{\pm}$. As χ varies from χ_- to χ_+, the function $I(\chi,\chi_-)$ varies from 0 and increases monotonically and finally tends to the resonance condition $I(\chi_+,\chi_-) = p\pi$. For $p=1$, $I(\chi,\chi_-)$ varies from 0 to π as χ varies from χ_- to χ_+, therefore, $\cos I(\chi,\chi_-)$ becomes an odd function with respect to χ. If we calculate the average of $g_o \cos I(\chi,\chi_-)=\cos\chi\ \cos I(\chi,\chi_-)+z\sin\chi\cos I(\chi,\chi_-)$ over $[\chi_-,\chi_+]$, the first odd function vanishes. This is why the bounce resonance ($p=1$) contribution in the central ideal region $z<<1$ is ignored in usual studies. The second even function, however, remains unvanished. This second term may be important in the outer inertial region $z>>1$.

Since $\sin\chi\cos I(\chi,\chi_-)/\left|v_{\parallel}\right|$ sharply tends to $-\infty$ as $\chi \to \chi_{\pm}$,the average of this function may be evaluated by the singular edge approximation. For $\chi \simeq \chi_-$, from the definition, the integral $I(\chi,\chi_-)$ may be approximately by

$$I(\chi,\chi_-) \simeq 2(\omega-\overline{\omega}_d)(\chi-\chi_-)^{\frac{1}{2}}(-2E\sin\chi_-)^{-\frac{1}{2}},$$

where $\sin\chi_-$ is determined from the turning point condition: $1-\lambda_0(1-\varepsilon\cos\chi)=0$. Making use of this approximation, we have the average from the second term:

$$g_o \cos I(\chi_+,\chi_-) \cong -\frac{2(E\epsilon\lambda_o)^{\frac{1}{2}}\sin\chi_-}{K_o Rq(\omega-\bar{\omega}_d)}\sin\left(\frac{2(\omega-\bar{\omega}_d)Rq}{(2E\epsilon\lambda_o\sin\chi_-)^{\frac{1}{2}}}\chi_+^{\frac{1}{2}}\right)z \qquad (10)$$

For deeply trapped state $\chi_+ \ll \pi$, this approximation shoud be accurate. When the argument of sin-function in eq.(10) is smaller than $\pi/2$, which may be satisfied for $E>2\epsilon^2/K^2_o$ for $\omega \cong \omega_b$(bounce frequency), eq.(10) may be approximated by $(2\chi_+\sin\chi_+)^{1/2}z/k$. The frequency ω obtained from the dispersion relation is much lower than ω_b as we shall see, this assumption may easily be satisfied. Since this average is proportional to z, it becomes important in the inertial region.

Introducing eq.(10) into eq.(8), and carrying out the energy integral for the same distribution function $F(E,\lambda)$ as in the derivation of eq.(9), we obtain for $p=1(\omega=\omega_b)$ resonance contribution in the form

$$U_t^1 \cong -(1+z^2)\bar{U}_t^1, \qquad (11)$$

where

$$\bar{U}_t = W_t\frac{\omega\omega_{bm}}{\omega_{bm}^2}\left[1+\left(\left(\frac{\omega}{\omega_{bm}}\right)^2-\frac{3}{2}\frac{\omega}{\omega_{bm}}\right)\log\left(1-\left(\frac{\omega_{bm}}{\omega}\right)^2\right)\right], \qquad (12)$$

$$W_t = \left(\frac{8q}{s\hat{B}k_o}\right)^2\chi_-\sin\chi_- p_h\Theta\left(\lambda_o-\frac{1}{1+\epsilon}\right), \qquad (13)$$

$\Theta(x)=1$ for $x>0$, otherwise $\Theta(x)=0$, and $\omega_{bm}=\omega_b(E_m)$. The term with the factor -3/2 in eq.(12) comes from $\partial F/\partial E$ as in eq.(9). From eq.(12), we find that the bounce resonance contribution U_t modifies the inertial coefficient Λ_c in eq.(3). Substituting eqs.(9) and (11) into eq.(3), we have a distilled ballooning mode equation.

$$\frac{d}{dz}f\frac{d\phi}{dz}-\left(U_o+\frac{U_t}{1+z^2}+\Lambda(1+z^2)\right)\phi=0, \qquad (14)$$

where the Mercier coefficient U_o and inertial coefficient Λ are modified by the trapped energetic partile effect in the form

$$U_o = U_c + U_t^o, \tag{15}$$

$$\Lambda = \Lambda_c + \overline{u_t^1}, \tag{16}$$

The coefficient U_1 remains unchanged. If we include the passing partlcle resonance contribution $U_p{}^1$, it modifies the inertial coefficent (16) in the same manner as $U_t{}^1$ does.

§3. Dispersion Relation

We proceed to the derivation of the eigenvalue condition for the distilled ballooning mode eq.(14) from the boundedness of the eigenfunction ϕ. Whithout the inertial coefficient, Λ-0. eq.(14) reduces to the Legendre differential equation whose solution is completely given by the Legendre function $P_\nu^\mu(iz)$ and $Q_\nu^\mu(iz)$, where μ and ν are related to the coefficient U_o and U_1 in the form [9]

$$\mu = (-U_1)^{\frac{1}{2}}, \tag{17}$$

$$\nu = -\frac{1}{2} + (\frac{1}{4} + U_o)^{\frac{1}{2}}, \tag{18}$$

From the bounded condition of the asymptotic solution: $P_\nu^\mu(iz)$ $=\Gamma(\nu+1/2)(2iz)^\nu/(\Gamma(\nu-\mu+1)\pi^{1/2})$ for $\nu>0$ and $z>>0$, the eigen value condition for the ideal ballooning mode has been given in the form $\mu = 1+\nu$ or

$$\frac{1}{2} + (\frac{1}{4} + U_o)^{\frac{1}{2}} = (-U_1)^{\frac{1}{2}}, \tag{19}$$

In eq.(19),the Mercier stability condition $1/4+U_o>0$ has been assumed. From eq.(15), the trapped energetic particle effect $U_t{}^o$ stabilizes the Mercier mode when $U_t{}^o>0$, while for $U_t{}^o<0$, it destabilizes.

When we have the inertial effect, Λ=0, the general solution of

eq.(14) is expressed in terms of the spheroidal functions[10]. The eigenvalue condition has also be given from the bounded condition of the solution in a general form. Instead of using the complicated general form, however, here we employ the methed in Ref.(7): In the inertial region, $z>>1$, eq.(14) reduces to the Bessel differntial equation whose solution can be expressed by [7] $(\pi/2z)^{1/2}K_\nu(iz)$ where K_ν is the modified Bessel function. In the region $z<<\Lambda^{-1/2}$, the solution of eq.(14) is given by the hypergeometric function: $\varphi=(1+z^2)^{-\mu/2}F((\nu-\mu)/2,-(\nu+\mu)/2,1/2,-z^2)$ for the even mode. Matching the asymptitic forms of these solutions, the eigenvalue condition for the even mode has been given in the form

$$(\frac{1}{2}\Lambda^{\frac{1}{2}})^{2\nu+1} = H(\mu,\nu), \tag{20}$$

where $H(\mu,\nu)$ is defined in terms of the gamma function:

$$H(\mu,\nu) = \frac{\Gamma(\frac{\mu-\nu}{2})\Gamma(-\frac{\nu+\mu}{2})\Gamma^2(\nu+\frac{1}{2})}{\Gamma(\frac{1+\nu+\mu}{2})\Gamma(\frac{1+\nu-\mu}{2})\Gamma^2(-\nu-\frac{1}{2})}, \tag{21}$$

Substituting eqs.(6) and (16) into the left hand side of eq.(20) the dispersion relation becomes

$$i(\frac{\Omega}{s})^2-\overline{U_t^1})^{\frac{1}{2}} = 2(H(\mu,\nu))^{\frac{1}{2\nu+1}}, \tag{22}$$

In eq.(22), the trapped particle effect in the central ideal region U_t^O is implicitly involved in the parameter ν through eqs.(15) and (18). Since the right hand side of eq.(22) comes from the fluid contribution, the pure bounce resonance excitation may be studied from the left hand side: $(\Omega/s)^2-\overline{U_t}=0$.

Behavior of the function $H(\mu,\nu)$ on (μ,ν) parameter space can be seen by a three demensional graphics in Fig.1. Due to the property of the gamma function, near the marginal stability condition (19), $\mu \simeq 1+\nu$, $H(\mu,\nu)$ is approximated in the form

$$H(\mu,\nu) \simeq C_B(\nu)(\mu - \nu - 1), \tag{23}$$

where the coefficient is given by

$$C_B(\nu) = \frac{(\nu+\frac{1}{2})\Gamma^3(\nu+\frac{1}{2})}{2\sqrt{\pi}\Gamma(\nu+1)}\cos\pi\nu. \tag{24}$$

Variation of the quantity $C_B(\nu)^{2/2\nu+1}$ as a function ν, as seen in Fig.2, is not so mild. When ν is small, it is approximated by

$$C_B(\nu)^{\frac{2}{2\nu+1}} = (\frac{\pi}{4})^2\{1-2\nu(2+3\psi(\frac{1}{2})-\psi(1)-\log\frac{\pi}{4})\} \simeq (\frac{\pi}{4})^2(1-5.7\nu),$$

where ψ is the pori-gamma function: $\psi(z)=d\log\Gamma(z)/dz$.

When ν is small, eq.(23) can be expressed by the fluid portion of energy $\delta W_f = \int_0^\infty dz\{(1+z^2)(d\phi_t/dz)^2 + (U_0 + U_1(1+z^2)^{-1})\phi_t^2\}$ with the trial function of the form $\varphi_t=(1+z^2)^{-1/2}$. In this case, $\delta W_f \simeq \nu+1-\mu$, and if we write $U_t^{-1}=\delta W_{kt}$, the dispersion relation (22) reduces to the same one treated in Ref.(5)

$$i(\Omega^2 - \delta W_{kt}^{-1})^{\frac{1}{2}} = \delta W_f. \tag{25}$$

The second term in the left hand side of eq.(25) is trapped particle bounce resonance contrbution instead of the transit resonance contribution in Ref.(4). From above argument, the dispersion relation of the form (25) may be valid for small ν and $\mu \simeq \nu+1$. This means that U_0 must be small which may correspond to the low-β plasma[6].

From eqs.(15) and (18), the relation between the Marcier coefficient and ν can be written by

$$\nu^2 + \nu = U_c + U_t^0. \tag{26}$$

If we separate the energetic particle effect Δ_h in the form $\nu=\nu_o+\Delta_h$ where ν_o is defined by $\nu_o^2+\nu_o=U_c$, the energetic effect is given by $\Delta_h \cong U_t^o/(1+2\nu_o)$. When ν_o is small again, we have $\Delta_h \cong U_t^o=\delta W_{kt}^o$. Therefore, including both δW_{kt}^o and δW_{kt}^1, the dispersion relation may be written in the form

$$i(\Omega^2-\delta W_{kt}^1)^{\frac{1}{2}}=\delta W_{kt}^o+\delta W_f. \qquad (27)$$

When δW_{kt}^1 and ω_*^i in Ω^2 are neglected, eq.(27) reduces to the one studied in Ref.(2).

We concentrate to the problem which remained to be studied, i.e., the bounce resonance excitation of the ballooning mode. For the sake of simplicity, we neglect δW_{kt}^o assuming $\omega_b >> \omega_d$. Introducing eq.(12) into eq.(22), we write the dispersion relation (22) in the form

$$D\cong\bar{\omega}^2+\gamma_o^2-\bar{W}_1\bar{\omega}[\bar{\omega}_{*m}+\bar{\omega}(\bar{\omega}_{*m}\bar{\omega}-\frac{3}{2})\log(1-\frac{1}{\bar{\omega}^2})]=0, \qquad (28)$$

where the bar over frequencies mean the normalization by the bounce frequency at the maximum energy ω_{bm}, $W_1=s^2\omega_A^2 W_1$, $\gamma_o^2=2s^2\omega_A^2 H(\mu,\nu)^{2\nu+1}$. When ν is small, $\bar{\omega}_i$ reduces to the ideal MHD growth rate $\bar{\omega}_i \cong \omega_A\delta W_f$. Contour graphics of γ_0=constant in the (α,s) parameter space is presented in Fig.3 near the marginal stability state $\gamma_0=0$ which corresponds to $\mu=\nu+1$.

§4. Result

We calculate the complex discrete root of eq.(28) in the complex ω-plane by the contour method making use of graphics of Mathematica[11]. An example of the "equi potential" contours of D =constant in the ω-

plane is presented in Fig.4. Some results are also examined by the two dimentional shooting method in a previous paper[4].

First we consider the ideal ballooning mode marginal stability state, i.e., the dispersion equation (28) without the fluid energy, $\gamma_O=0$. In this case, we can study the existence of pure bounce resonant mode.

So far the $\partial F/\partial E$ in Q in eq.(8), which is the source of energetic particle free energy in velocity space, has been neglected in the resonance theories[1)2)3)12)]. Here we consider the effect of this term in the resonance problem. For the simple slowing down distribution F being proportional to $E^{-3/2}$, this term which reduced to the term with the factor -3/2 in eq.(28) may stabilize the resonant mode as in the drift resonance problem[8)]. Precisely speaking, the energetic particle distribution should be determined self consistently[12)] from a generalized Fokker-Plank equation which includes both source and dissipations due to classical and anomalous transport prosesses induced by the resonant mode instability. Here we employ the simple slowing down model to see how the term $\partial F/\partial E$ stabilize or destabilizes the resonant mode.

The normalized growth rates with and without $\partial F/\partial E$ term are compared in Fig.5 where the solid and broken curves represent the case without and with $\partial F/\partial E$ term, respectively. There is a threshold W^*_1 above which the resonant mode becomes unstable. The normalized frequencies for both cases are also plotted as functions of the energetic particle contribution $\bar{W}$ in Fig.5. Notice that the mode still exists even below the threshold $\bar{W}<W^*_1$ as a stationary oscillating mode. The threshold W^*_1 as a function of $\bar{\omega}_{*n}$ is plotted in Fig.6. The resonant mode is unstable above these curves. As seen in Figs.5 and 6, the stabilization by $\partial F/\partial E$ is significant, although our simple

model distribution function may over stabilize the mode because $\partial F/\partial E<0$ in the whole energy region.

Here we briefly consider one of the simplest case of $\omega_{*m}=0$. In this case, the source of free energy comes only from the fluid energy which is stabilized by $\partial F/\partial E$ of the slowing down distribution, and eq.(28) reduces to

$$\bar{\omega}^2+\gamma_o^2+\frac{3}{2}\bar{\omega}^2\bar{W}_1\log(1-\frac{1}{\bar{\omega}^2})=0, \qquad (29)$$

When $\gamma_0=0$, i.e., at the marginal stability state of the ideal mode, eq.(29) is solved analyticaly:

$$\bar{\omega}_i=0, \qquad \bar{\omega}_r=(1-e^{-\frac{2}{3\bar{W}_1}})^{-\frac{1}{2}}.$$

which is a stationary oscillating mode with $\bar{\omega}_r>1$. When γ_O is small, i.e., close to the ideal ballooning marginal state, eq.(29) is approximately solved in the form

$$\bar{\omega}_i\cong\gamma_o(1+\frac{3}{2}\bar{W}_1\log\gamma_o),$$

which increases as $W_1\to0$, and tends to the ideal growth rate γ_O.

Finally we calculate the dispersion equation (28) including both γ_O and $\bar{\omega}_{*m}$. For $\omega_{*m}=-\omega_{bm}$, variations of discrete root of eq.(28) in the complex ω-plane are presented in Fig.7 for various values of γ_0 and $\bar{W}$. When $W_1\to0$ in Fig.7, the real part $\bar{\omega}_r$ tends to zero and the imaginary part $\bar{\omega}_i$ tends to the ideal MHD growth rate γ_0 as in the case of drift resonance problem[13)14)]. Without $\partial F/\partial E$ term (solid curves), the transition from the MHD mode to the resonant mode occurs continuously as $\bar{W}$ increases as in the case of $\gamma_O=0$. With the slowing down stabilization $\partial F/\partial E=0$, variations of $\bar{\omega}_i$ and $\bar{\omega}_r$ changed as shown by the dotted curves in Fig.7.

When $\omega_{*m}=\omega_{bm}$, i.e., the spatial gradient of F changes its direction, which may occur in the central region for the deeply trapped

particles, all results change approximately symmetrically with respect to the imaginary axis $\omega_i=0$.

Variations of $\bar{\omega}_i$ as function of $\bar{W}$ are plotted for different values of γ_0 in Fig.8, where the comparision is made with the case of $\partial F/\partial E* 0$ whose result is shown by dotted curves. When $\partial F/\partial E* 0$, the growth rate $\bar{\omega}_i$ is always smaller than the "ideal" one γ_0 as shown by the broken curves. One will see how $\partial F/\partial E$ is important in the stabilization of the resonant mode. This effect, however, has been neglected in the p=0 resonance studies[3)5)] assuming $\omega_{*m}>>\omega_{dm}$.

AS $\bar{W}$ increases, pure oscillating branch on the real axis $\bar{\omega}_i=0$ suddenly appears, i.e., a bifurcation of the discrete root happens. This branching of $\bar{\omega}_r$ is shown for the case of $\gamma_0=0.05$ in Fig.9. At certain value of $\bar{W}$, the real frequency $\bar{\omega}_r$ sprits into two branches. The upper branch is the stationary oscillating mode, whose frequency is much lower than lower branch's, while the lower branch is the resonant mode.

§5. Summary

A dispersion equation is derived from the bounded condition of analytical eigenfunctions of the averaged ballooning mode equation which includes the kinetic effect of trapped energetic particles in a toroidal plasma with the circular magnetic surface cross section. The kinetic energy integral is evaluated for the p=0 precessional drift resonance and p=1 bounce resonance in the case of the simple model slowing down distribution function.

The drift resonance integral modifies the Mercier coefficient, and is involved in the dispersion equation in a complicated manner through the gamma function as indicated in eq.(21). Near the ideal ballooning mode marginal stability state, the dispersion equation is

reduced to the simple one derived from the energy principle.

Although the trapped particle bounce resonance integral vanishes on the average in the central ideal region, it remains unvanished in the outer inertial region and play an important role for the bounce resonance excitation of the ballooning mode. Detailed behavior of the bounce resonant mode is studied by numerically calculating the dispersion equation. The term $\partial F/\partial E$ in the kinetic bounce resonance integral for the slowing down distribution is found to stabilize the resonant mode as in the p=0 drift resonant case[8]. The model of the distribution function F used here, however, may be too simple to be realistic. If we take into account the dissipation due to instabilities, F may suffer change. The distribution F should be determined in a self consistent manner, which remines to be investigated.

From numerical results, as the energetic particle effect $\bar{W}_i$ is increased, a bifurcation of the MHD mode into the resonant mode and stationary oscillationg mode is also found.

Acknowledgement

The author would like to thank Dr. C.Z. Cheng and Prof. H. Akimune for helpful discussion. He is also grateful to Prof. T. Amano for providing information about Mathematica. This study was a joint research program in National Institute of Fusion Science.

References

1) M.N.Rosenbluth,S.Tsai,J.W.Van Dam and M.G.Engquist: Rhys.Rev.Lett. **51**(1983)1967.

2) J.Wieland and L.Chen:Phys.Fluids **28**(1985)1359.

3) L.Chen,R.B.White and N.M.Rosenbluth:Phys.Rev.Lett. **52** (1984)1122.

4) T.Yamagishi:J.Phys.Soc.Jpn. **59**(1990)138.

5) L.Chen:Princeton Plasma Physics Laboratory Report PPPL-2597(1989).

6) A.B.Mikhailovskii,S.V.Novakovaskii,and S.E.Shafranov: Sov.J.Plasma Phys. **13**(1987)749.

7) T.M.Antonsen,Jr.,A.Ferreira and J.J.Ramos:Plasma Physics **29**(1982)197.

8) T.Yamagishi:Annual Report in National Institute of Fusion Science 1990.

9) A.B.Mikhailovskii,S.V.Novakovaskii,and A.I.Smolyokov: Sov.J.Plasma Physics **14**(1988)830.

10) R.B.Paris,N.Auby:J.Math.Phys. **27**(1986)2188.

11) S.Wolfram:Mathematica,A system for Doing Mathematics by Computer, Addison-Wesley Publishing Co.,New York,1988.

12) H.L.Berk and B.N.Breizman:Phys. Fluids B2(1990)2226.

13) Y.Z.Zhang,H.L.Berk and S.M.Mahajan:Nuclear Fusion, **29**(1989)848.

14) T.Yamagishi:submitted to Nucl.Fusion (1990).

Figures Captions

Fig.1: Three dimensional surface graphics of dispersion function $H(\mu,\nu)$. The line $\mu=\nu+1$ on which $H(\mu,\nu)=0$ indicates the balloonibg mode marginal stability state.

Fig.2: Variation of coefficient of dispersion function $C_B^{2/(2\nu+1)}$ as a function of ν.

Fig.3: Contour graphics of fluid contribution γ_O in (s,α)-plane.

Fig.4: Equipotential contour graphics of complex dispersion function D for $\gamma_O^2=0.1$ and $\bar{W}=0.22$. Each center of contours give root of D=0.

Fig.5: Variation of normalized growth rate ω_i/ω_{bm} of bounce resonant mdoe as a function of $\bar{W}$ for ideal ballooning mode marginal stability state $\gamma_O = 0$. Broken curve represents the case with $\partial F/\partial E$.

Fig.6: Theshold W^*_1 as a function of ω_{*m} for $\gamma_O = 0$. Broken curve represents the case with $\partial F/\partial E$.

Fig.7: Variations of discrete roots $\bar{\omega}_i$ and $\bar{\omega}_r$ for various values of γ_O and $\bar{W}$. Broken curves represent the case with $\partial F/\partial E$.

Fig.8: Behavior of normalized growth rate ω_i/ω_{bm} as function of $\bar{W}$ for $\omega_{*m} = -\omega_{bm}$. Broken curve represent the case with $\partial F/\partial E$.

Fig.9:Behavior of normalized frequency ω_r/ω_{bm} as function of $\bar{W}$ for $\omega_{*m} = -\omega_{bm}$.

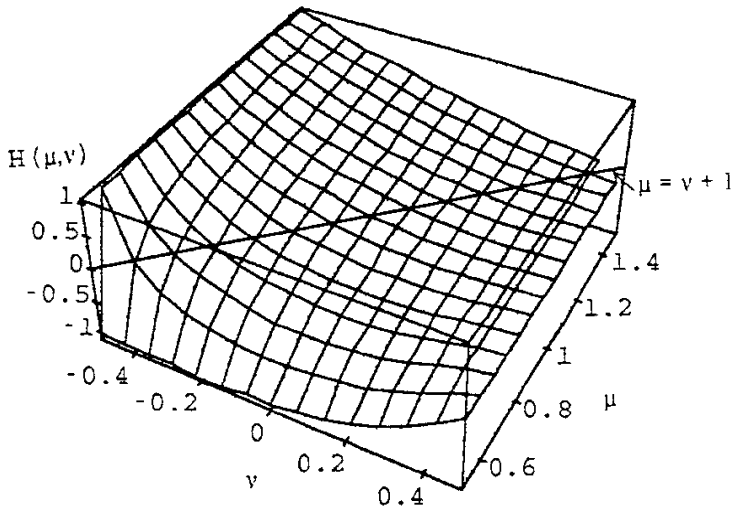
H(μ,ν)
1
0.5
0
-0.5
-1
-0.4
-0.2
0
0.2
0.4
ν
μ = ν + 1
1.4
1.2
1
0.8
0.6
μ

Fig.1

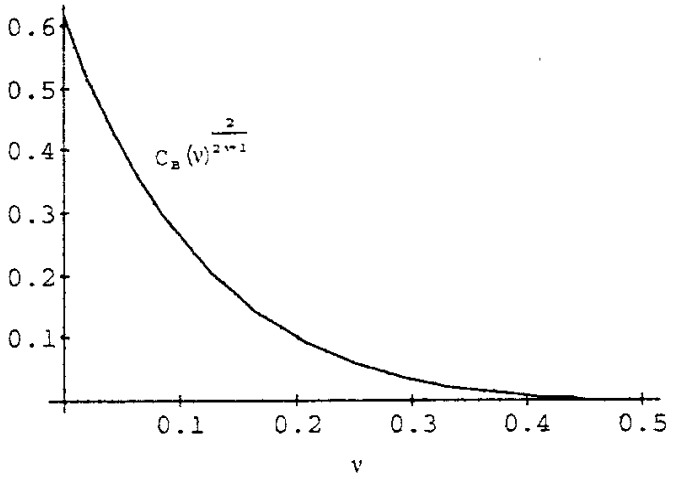
0.6
0.5
0.4
0.3
0.2
0.1
$C_B(\nu)^{\frac{2}{2\nu-1}}$
0.1
0.2
0.3
0.4
0.5
ν

Fig.2

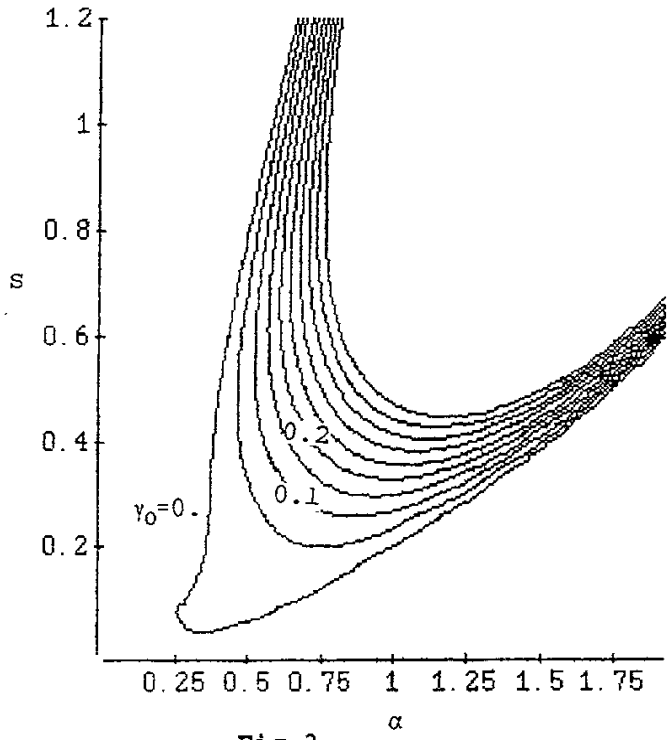
1.2
1
0.8
S
0.6
0.4
0.2
γ_0=0.
0.2
0.1
0.25 0.5 0.75 1 1.25 1.5 1.75
α

Fig.3

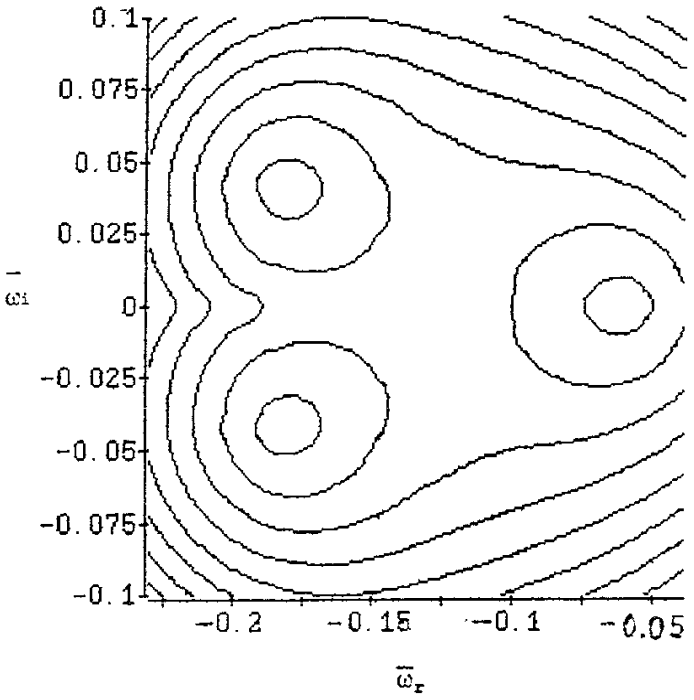
0.1
0.075
0.05
0.025
0
-0.025
-0.05
-0.075
-0.1
$\bar{\omega}_i$
-0.2 -0.15 -0.1 -0.05
$\bar{\omega}_r$

Fig.4

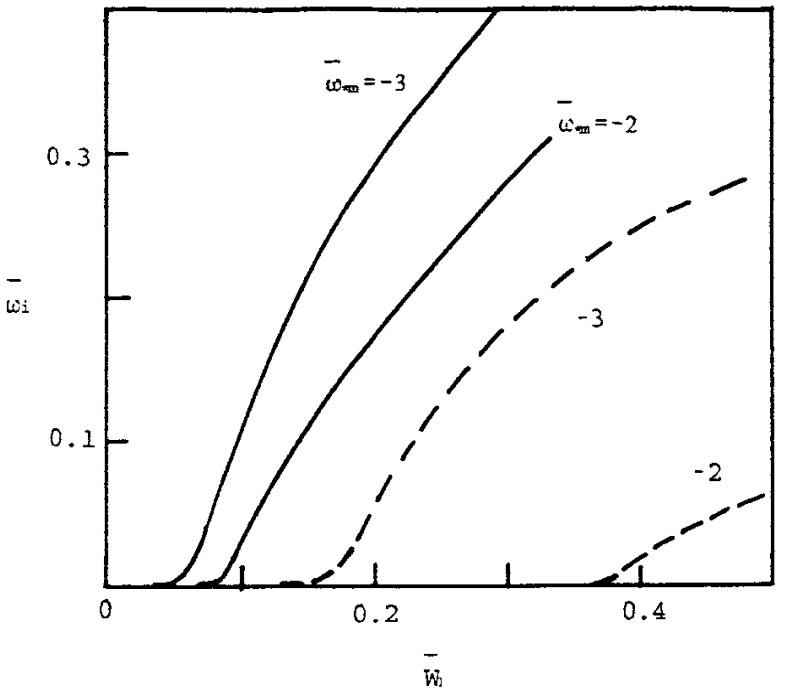
$\bar{\omega}_{wm}=-3$
$\bar{\omega}_{wm}=-2$
0.3
0.1
$\bar{\omega}_i$
-3
-2
0
0.2
0.4
$\bar{W}_i$

Fig.5

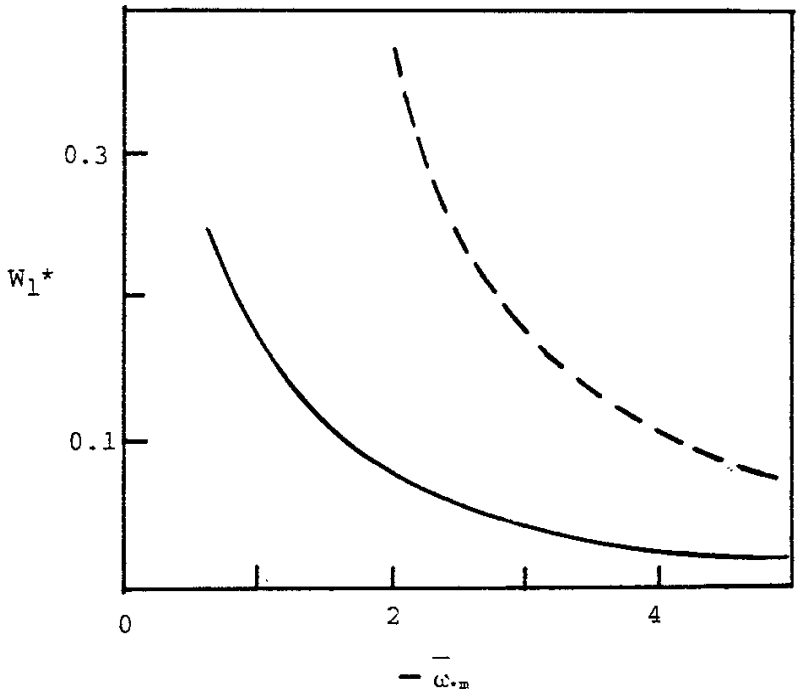
0.3
0.1
W_1^*
0
2
4
$-\bar{\omega}_{*m}$

Fig.6

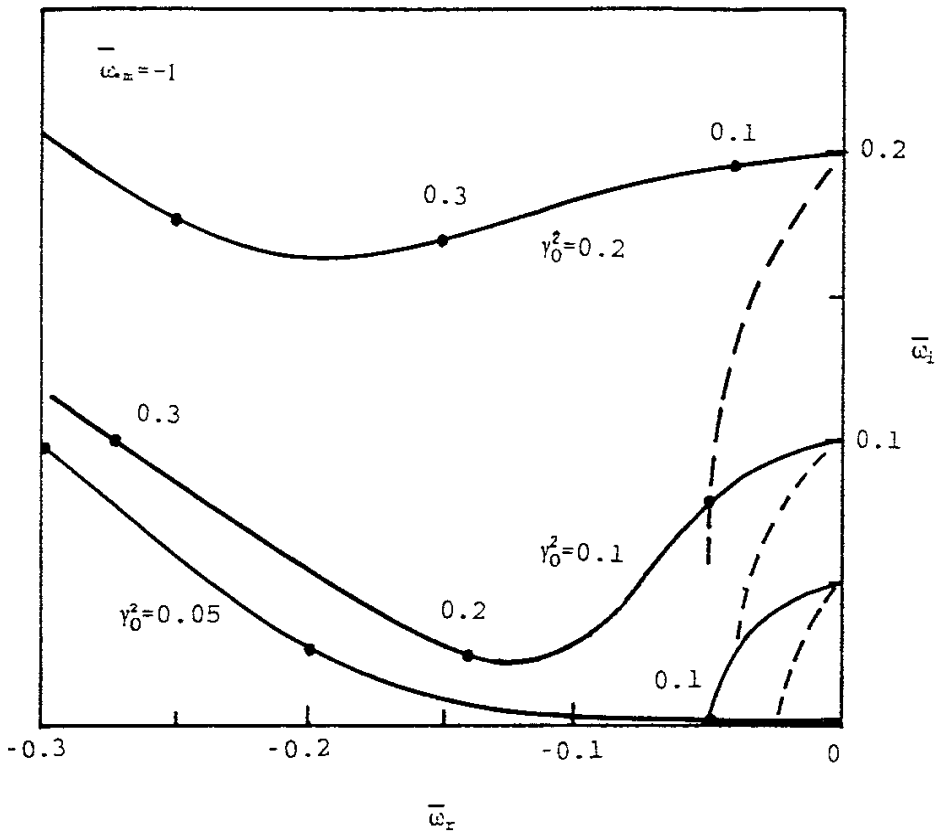
$\bar{\omega}_m = -1$
0.1
0.2
0.3
$\gamma_0^2 = 0.2$
$\bar{\omega}_i$
0.3
0.1
$\gamma_0^2 = 0.1$
$\gamma_0^2 = 0.05$
0.2
0.1
-0.3
-0.2
-0.1
0
$\bar{\omega}_r$

Fig.7

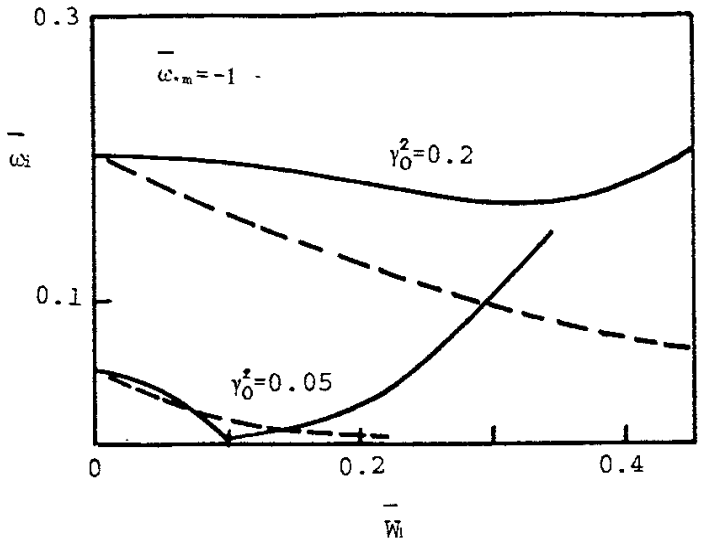
0.3
$\bar{\omega}_{sm}=-1$
$\bar{\omega}_i$
$\gamma_0^2=0.2$
0.1
$\gamma_0^2=0.05$
0
0.2
0.4
$\bar{W}_1$

Fig.8

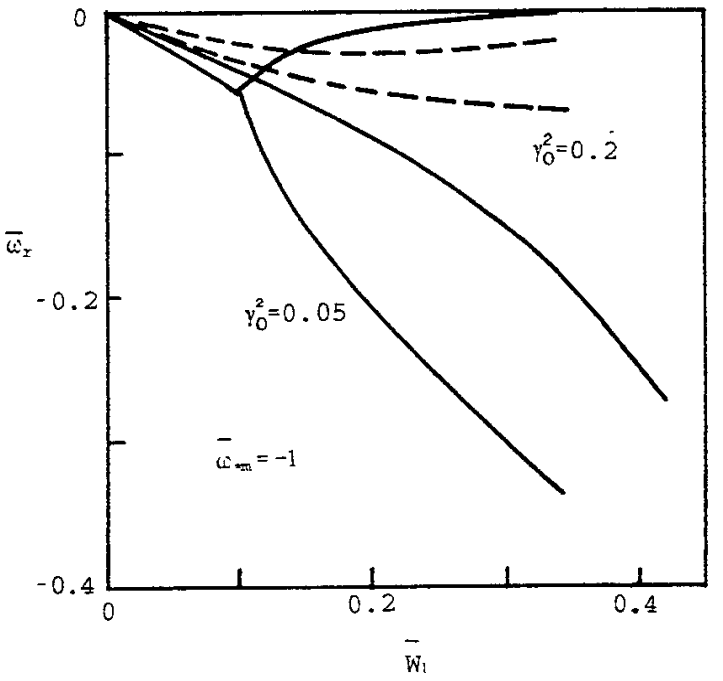
0
$\gamma_0^2=0.2$
$\bar{\omega}_r$
-0.2
$\gamma_0^2=0.05$
$\bar{\omega}_{sm}=-1$
-0.4
0
0.2
0.4
$\bar{W}_1$

Fig.9

Recent Issues of NIFS Series

NIFS-26 K. Ida, S. Hidekuma, Y. Miura, T. Fujita, M. Mori, K. Hoshino, N. Suzuki, T. Yamaguchi and JFT-2M Group, *Edge Electron Field Profiles of H-mode Plasmas in JFT-2M Tokamak* ; Apr. 1990

NIFS-27 N. Nakajima and M. Okamoto, *Beam-Driven Currents in the 1/ v Regime in a Helical System* ; Apr. 1990

NIFS-28 K. Itoh, K. Nagasaki and S.I. Itoh, *Heat Deposition on the Partial Limiter* ; Apr. 1990

NIFS-29 S.-I. Itoh A. Fukuyama adn K. Itoh, *Fokker-Plank Equation in the Presence of Anomallous Diffusion* ; May. 1990

NIFS-30 K. Yamazaki, O. Motojima, M. Asao, M. Fujiwara and A. Iiyoshi, *Design Scalings and Optimizations for Super-Conducting Large Helical Devices* ; May 1990

NIFS-31 H. Sanuki, T. Kamimura, K. Hanatani, K. Itoh and J. Todoroki, *Effects of Electric Field on Particle Drift Orbits in a l =2 Torsatron* ; May 1990

NIFS-32 Yoshi H. Ichikawa, *Experiments and Applications of Soliton Physics*; June 1990

NIFS-33 S.-I. Itoh, *Anomalous Viscosity due to Drift Wave Turbulence* ; June 1990

NIFS-34 K. Hamamatsu, A. Fukuyama, S.-I. Itoh, K. Itoh and M. Azumi, *RF Helicity Injection and Current Drive* ; July 1990

NIFS-35 M. Sasao, H. Yamaoka, M. Wada and J. Fujita, *Direct Extraction of a Na- Beam from a Sodium Plasma* ; July 1990

NIFS-36 N. Ueda, S.-I. Itoh, M. Tanaka and K. Itoh, *A Design Method of Divertor in Tokamak Reactors* Aug. 1990

NIFS-37 J. Todoroki, *Theory of Longitudinal Adiabatic Invariant in the Helical Torus*; Aug. 1990

NIFS-38 S.-I. Itoh and K. Itoh, *Modelling of Improved Confinements – Peaked Profile Modes and H-Mode–* ; Sep. 1990

NIFS-39 O. Kaneko, S. Kubo, K. Nishimura, T. Syoji, M. Hosokawa, K. Ida, H. Idei, H. Iguchi, K. Matsuoka, S. Morita, N. Noda, S. Okamura, T. Ozaki, A. Sagara, H. Sanuki, C. Takahashi, Y. Takeiri, Y. Takita, K. Tsuzuki, H. Yamada, T. Amano, A. Ando, M. Fujiwara, K. Hanatani, A. Karita, T. Kohmoto, A. Komori, K. Masai, T. Morisaki, O. Motojima, N. Nakajima, Y. Oka, M. Okamoto,

S. Sobhanian and J. Todoroki, *Confinement Characteristics of High Power Heated Plasma in CHS*; Sep. 1990

NIFS-40 K. Toi, Y. Hamada, K. Kawahata, T. Watari, A. Ando, K. Ida, S. Morita, R. Kumazawa, Y. Oka, K. Masai, M. Sakamoto, K. Adati, R. Akiyama, S. Hidekuma, S. Hirokura, O. Kaneko, A. Karita, T. Kawamoto, Y. Kawasumi, M. Kojima, T. Kuroda, K. Narihara, Y. Ogawa, K. Ohkubo, S. Okajima, T. Ozaki, M. Sasao, K. Sato, K.N. Sato, T. Seki, F. Shimpo, H. Takahashi, S. Tanahashi, Y. Taniguchi and T. Tsuzuki, *Study of Limiter H- and IOC- Modes by Control of Edge Magnetic Shear and Gas Puffing in the JIPP T-IIU Tokamak*; Sep. 1990

NIFS-41 K. Ida, K. Itoh, S.-I. Itoh, S. Hidekuma and JIPP T-IIU & CHS Group, *Comparison of Toroidal/Poloidal Rotation in CHS Heliotron/Torsatron and JIPP T-IIU Tokamak*; Sep .1990

NIFS-42 T.Watari, R.Kumazawa,T.Seki, A.Ando,Y.Oka, O.Kaneko, K.Adati, R.Ando, T.Aoki, R.Akiyama, Y.Hamada, S.Hidekuma, S.Hirokura, E.Kako, A.Karita, K.Kawahata, T.Kawamoto, Y.Kawasumi, S.Kitagawa, Y.Kitoh, M.Kojima, T. Kuroda, K.Masai, S.Morita, K.Narihara, Y.Ogawa, K.Ohkubo, S.Okajima, T.Ozaki, M.Sakamoto, M.Sasao, K.Sato, K.N.Sato, F.Shinbo, H.Takahashi, S.Tanahashi, Y.Taniguchi, K.Toi, T.Tsuzuki, Y.Takase, K.Yoshioka, S.Kinoshita, M.Abe, H.Fukumoto, K.Takeuchi, T.Okazaki and M.Ohtuka, *Application of Intermediate Frequency Range Fast Wave to JIPP T-IIU and HT-2 Plasma*; Sep. 1990

NIFS-43 K.Yamazaki, N.Ohyabu, M.Okamoto, T.Amano, J.Todoroki, Y.Ogawa, N.Nakajima, H.Akao, M.Asao, J.Fujita, Y.Hamada, T.Hayashi, T.Kamimura, H.Kaneko, T.Kuroda, S.Morimoto, N.Noda, T.Obiki, H.Sanuki, T.Sato, T.Satow, M.Wakatani, T.Watanabe, J.Yamamoto, O.Motojima, M.Fujiwara, A.Iiyoshi and LHD Design Group, *Physics Studies on Helical Confinement Configurations with l=2 Continuous Coil Systems*; Sep. 1990

NIFS-44 T.Hayashi, A.Takei, N.Ohyabu, T.Sato, M.Wakatani, H.Sugama, M.Yagi, K.Watanabe, B.G.Hong and W.Horton, *Equilibrium Beta Limit and Anomalous Transport Studies of Helical Systems*; Sep. 1990

NIFS-45 R.Horiuchi, T.Sato, and M.Tanaka, *Three-Dimensional Particle Simulation Study on Stabilization of the FRC Tilting Instability*; Sep. 1990

NIFS-46 K.Kusano, T.Tamano and T. Sato, *Simulation Study of Nonlinear Dynamics in Reversed-Field Pinch Configuration*; Sep. 1990

NIFS-47 Yoshi H.Ichikawa, *Solitons and Chaos in Plasma*; Sep. 1990

NIFS-48 T.Seki, R.Kumazawa, Y.Takase, A.Fukuyama, T.Watari, A.Ando, Y.Oka, O.Kaneko, K.Adati, R.Akiyama, R.Ando, T.Aoki, Y.Hamada, S.Hidekuma, S.Hirokura, K.Ida, K.Itoh, S.-I.Itoh, E.Kako, A. Karita, K.Kawahata, T.Kawamoto, Y.Kawasumi, S.Kitagawa, Y.Kitoh, M.Kojima, T.Kuroda, K.Masai, S.Morita, K.Narihara, Y.Ogawa, K.Ohkubo, S.Okajima, T.Ozaki, M.Sakamoto, M.Sasao, K.Sato, K.N.Sato, F.Shinbo, H.Takahashi, S.Tanahashi, Y.Taniguchi, K.Toi and T.Tsuzuki, *Application of Intermediate Frequency Range Fast Wave to JIPP T-IIU Plasma*; Sep.1990

NIFS-49 A.Kageyama, K.Watanabe and T.Sato, *Global Simulation of the Magnetosphere with a Long Tail: The Formation and Ejection of Plasmoids*; Sep.1990

NIFS-50 S.Koide, *3-Dimensional Simulation of Dynamo Effect of Reversed Field Pinch*; Sep. 1990

NIFS-51 O.Motojima, K. Akaishi, M.Asao, K.Fujii, J.Fujita, T.Hino, Y.Hamada, H.Kaneko, S.Kitagawa, Y.Kubota, T.Kuroda, T.Mito, S.Morimoto, N.Noda, Y.Ogawa, I.Ohtake, N.Ohyabu, A.Sagara, T. Satow, K.Takahata, M.Takeo, S.Tanahashi, T.Tsuzuki, S.Yamada, J.Yamamoto, K.Yamazaki, N.Yanagi, H.Yonezu, M.Fujiwara, A.Iiyoshi and LHD Design Group, *Engineering Design Study of Superconducting Large Helical Device*; Sep. 1990

NIFS-52 T.Sato, R.Horiuchi, K. Watanabe, T. Hayashi and K.Kusano, *Self-Organizing Magnetohydrodynamic Plasma*; Sep. 1990

NIFS-53 M.Okamoto and N.Nakajima, *Bootstrap Currents in Stellarators and Tokamaks*; Sep. 1990

NIFS-54 K.Itoh and S.-I.Itoh, *Peaked-Density Profile Mode and Improved Confinement in Helical Systems*; Oct. 1990

NIFS-55 Y.Ueda, T.Enomoto and H.B.Stewart, *Chaotic Transients and Fractal Structures Governing Coupled Swing Dynamics*; Oct. 1990

NIFS-56 H.B.Stewart and Y.Ueda, *Catastrophes with Indeterminate Outcome*; Oct. 1990

NIFS-57 S.-I.Itoh, H.Maeda and Y.Miura, *Improved Modes and the Evaluation of Confinement Improvement*; Oct. 1990

NIFS-58 H.Maeda and S.-I.Itoh, *The Significance of Medium- or Small-size Devices in Fusion Research*; Oct. 1990

NIFS-59 A.Fukuyama, S.-I.Itoh, K.Itoh, K.Hamamatsu, V.S.Chan, S.C.Chiu, R.L.Miller and T.Ohkawa, *Nonresonant Current Drive by RF Helicity Injection*; Oct. 1990

NIFS-60 K.Ida, H.Yamada, H.Iguchi, S.Hidekuma, H.Sanuki, K.Yamazaki and CHS Group, *Electric Field Profile of CHS Heliotron/Torsatron Plasma with Tangential Neutral Beam Injection*; Oct. 1990

NIFS-61 T.Yabe and H.Hoshino, *Two- and Three-Dimensional Behavior of Rayleigh-Taylor and Kelvin-Helmholz Instabilities*; Oct. 1990

NIFS-62 H.B. Stewart, *Application of Fixed Point Theory to Chaotic Attractors of Forced Oscillators;* Nov. 1990

NIFS-63 K.Konn., M.Mituhashi, Yoshi H.Ichikawa,*Soliton on Thin Vortex Filament;* Dec. 1990

NIFS-64 K.Itoh, S.-I.Itoh and A.Fukuyama,*Impact of Improved Confinement on Fusion Research;* Dec. 1990

NIFS -65 A.Fukuyama, S.-I.Itoh and K. Itoh,*A Consistency Analysis on the Tokamak Reactor Plasmas;* Dec. 1990

NIFS-66 K.Itoh, H. Sanuki, S.-I. Itoh and K. Tani,*Effect of Radial Electric Field on α-Particle Loss in Tokamaks;* Dec. 1990

NIFS-67 K.Sato,and F.Miyawaki,*Effects of a Nonuniform Open Magnetic Field on the Plasma Presheath*; Jan.1991

NIFS-68 K.Itoh and S.-I.Itoh,*On Relation between Local Transport Coefficient and Global Confinement Scaling Law;* Jan. 1991

NIFS-69 T.Kato, K.Masai, T.Fujimoto,F.Koike, E.Källne, E.S.Marmar and J.E.Rice,*He-like Spectra Through Charge Exchange Processes in Tokamak Plasmas;* Jan.1991

NIFS-70 K. Ida, H. Yamada, H. Iguchi, K. Itoh and CHS Group, *Observation of Parallel Viscosity in the CHS Heliotron/Torsatron* ; Jan.1991

NIFS-71 H. Kaneko, *Spectral Analysis of the Heliotron Field with the Toroidal Harmonic Function in a Study of the Structure of Built-in Divertor* ; Jan. 1991

NIFS-72 S. -I. Itoh, H. Sanuki and K. Itoh, *Effect of Electric Field Inhomogeneities on Drift Wave Instabilities and Anomalous Transport* ; Jan. 1991

NIFS-73 Y.Nomura, Yoshi.H.Ichikawa and W.Horton,*Stabilities of Regular Motion in the Relativistic Standard Map;* Feb. 1991

NIFS-74 T.Yamagishi, *;Electrostatic Drift Mode in Toroidal Plasma with Minority Energetic Particles,* Feb. 1991